Polymer 65 (2015) 193–201

Contents lists available at ScienceDirect

Polymer

journal homepage: www.elsevier.com/locate/polymer

Synthesis and characterization of two new benzothiadiazole- and fused bithiophene based low band-gap D–A copolymers: Application as donor bulk heterojunction polymer solar cells

M.L. Keshtov [a, **], G.D. Sharma [c, *], S.A. Kuklin [a], I.E. Ostapov [b], D.Yu. Godovsky [a], A.R. Khokhlov [a, b], F.C. Chen [d]

[a] Institute of Organoelement Compounds of the Russian Academy of Sciences, Vavilova St., 28, 119991 Moscow, Russian Federation
[b] Lomonosov Moscow State University, Faculty of Physics, 1-2 Leninskiye Gory, Moscow 119991, Russian Federation
[c] R & D Center for Engineering and Science, JEC Group of Colleges, Jaipur Engineering College, Kukas, Jaipur 303101, India
[d] Department of Photonics, National Chiao Tung University, Hsinchu, Taiwan 300, Taiwan, ROC

ARTICLE INFO

Article history:
Received 11 December 2014
Received in revised form
20 March 2015
Accepted 21 March 2015
Available online 28 March 2015

Keywords:
D–A copolymers
Bulk heterojunction solar cells
Power conversion efficiency

ABSTRACT

Two new narrow bandgap D–A conjugated copolymers **P1** and **P2** containing different fused thiophene donor unit and same benzothiadiazole acceptor unit were synthesized by Stille cross-coupling polymerization, and characterized by ^{1}H NMR, elemental analysis and GPC, TGA, DSC. Cyclic voltammetry measurement showed that the HOMO energy level both copolymers is deep lying (−5.10 and −5.35 eV for **P1** and **P2**, respectively) which show that copolymers has good stability in the air and assured a higher open circuit voltage when it photovoltaic application. These copolymer were used as donor along with $PC_{71}BM$ and the BHJ polymer solar cells based on **P1**:$PC_{71}BM$ and **P2**:$PC_{71}BM$ processed with chloroform (CF) solvent showed over all PCE of 4.54% and 4.36%, respectively. Additionally, the PCE was improved up to 5.62% and 5.24% for **P1**:$PC_{71}BM$ and **P2**:$PC_{71}BM$ active layer processed with DIO (4 v%)/CF solvent. The enhancement in the PCE has been attributed to improved nanoscale morphology and crystalline nature of active layer as well as charge transport in the device with the addition of DIO, due to the higher boiling point of DIO causing slow evaporation rate during the film formation.

1. Introduction

Organic solar cells (OSCs) based on the bulk heterojunction active layers consist of electron donating polymers and electron accepting fullerene derivatives have attracted significant attention due to their low cost of fabrication using convenient roll to roll printing techniques and light weight devices [1]. Remarkable progress has been made in improving the power conversion efficiencies of OSCs based on single BHJ have surpassed 8% [2] and the PCE of tandem OSC has broken 10% [3]. To improve the PCE further, significant efforts have been made to increase the short circuit current (J_{sc}), fill factor (FF) and open circuit voltage (V_{oc}) of the OSCs. The V_{oc} of the OSCs directly related to the energy difference of highest unoccupied molecular orbital (HOMO) of donor and lowest occupied molecular orbital (LUMO) of acceptor energy levels. To increase the V_{oc}, strategies have been focused on the synthesis of new polymers and/or new acceptors to achieve optimal donor (D)–acceptor (A) energy level offsets [4]. In order to achieve high J_{sc} of OSCs conjugated polymers are required to have a broad light absorption spectrum that effectively overlaps the solar spectrum for effective exciton generation, high charge carrier mobility of donor and acceptor materials, for efficient charge transport and collection. Among the various conjugated polymers that can be used for BHJ-OSCs, donor–acceptor (D–A) type conjugated copolymers have been recently identified as promising candidate for the use in OSCs due to their broad light absorption spectrum [5] and strong intermolecular interactions, which facilitate charge generation and transport [6]. In a D–A polymer system, the intra- and intermolecular interactions between the D and A units can lead to self assembly into ordered structures and strong π-stacking of polymer chains, which favor charge carrier transport [7]. In this approach, both HOMO/LUMO energy levels and the bandgap of D–A polymers can

* Corresponding author. Tel.: +91 1426 227345; fax: +91 1426 511240.
** Corresponding author.
E-mail addresses: keshtov@ineos.ac.ru (M.L. Keshtov), sharamgd_in@yahoo.com, gdsharma273@gmail.com (G.D. Sharma).

http://dx.doi.org/10.1016/j.polymer.2015.03.058
0032-3861/

be effectively tuned by using a combination of various types of D and A units having different electron donating and electron withdrawing strengths via intramolecular charge transfer. Moreover, the different structure and solubilizing groups of D and A can change other properties such as molecular packing and solubility [8].

The ideal D–A polymer should have a combination of weak donor and strong acceptor units, in which weak donor helps maintain a low HOMO level whereas strong acceptor would reduce the band gap of the polymer [9]. Among the various D–A conjugated polymers building blocks, 2, 1, 3-benzothiazole (BT) as acceptor unit, due to its easy preparation, excellent stability and electro-optical characteristics together with its ability to adopt a quinoid structure. A D–A polymer with BT derivative as electron withdrawing unit in which two thiophene moieties (DTBT) were flanked into the benzene ring of BT as a π-bridge for reducing steric hindrance and tuning the electronic properties can also be ideal donor material of high performance OSCs. In recent years, benzotrithiophenes (BTT) have emerged as attractive donor units for the designing of D–A polymers which showed promising performance in both OFETs and polymer solar cells [7a]. This kind of donors possesses high coplanarity and extended π-conjugation, which should promote intermolecular π-stacking and charge transport in BTT containing polymers.

In order to accomplish this task new approach to make the π-conjugated polymers was realized based on one and the same structure of macromolecule (strong alternation of donor and acceptor fragments, quinoid character of π-conjugation, planarity). In view of the above mentioned new effective synthetic pathway to obtain new class of fused thiophene containing monomers with increased quinoid character of π-conjugation and basing on such monomers by selection of structural types, their composition and sequence of alternation the conditions for directed synthesis of low band gap π-conjugated polymers were realized.

In this study, we have synthesized two benzothiadiazole- and fused bithiophene D–A copolymers **P1** and **P2** with same acceptor moiety and different donor units i. e. 2,8-Dibromo-4,6-bis(n-octylthiophen-2-yl) benzo[2,1-*b*:3,4-*b*′:5,6-*c*″] trithiophene and 2,5-dibrom-8-heptodecyl-10N-bisthieno [2′,3′:6,7; 3″,2″:4,5] indeono[1,2-d][1,3] thiazole for **P1** and **P2**, respectively. The later donor is weak as compared to former. These donor monomers contains highly fused thiophene unit and can form π–π stacked structure, which is favorable for increasing charge carrier mobility and morphology of the resulted film cast from the solution processing, which are very important for polymer solar cells. Similar monomers are synthesized by Mullen and used them for field effect transistor devices [7] and reported high charge carrier mobility. In addition, Mullen et al. prepared this monomers in 7 stages (starting from 2,2′-bithiophene) and the target monomers were obtained in only 18% yield (by the Rh − catalyzed cyclization). In our synthetic scheme there are 6 stages (starting from bithiophene) and the maximum yield on the cyclization stage is achieved of 72–73%. In addition, our synthetic stages are simpler and easily scalable to large loading of starting materials. We modified structure of monomers by introducing alkylthiophene fragments for increasing charge carrier mobility, since it's known that mobility is important for OSC too. The device based on **P1**:$PC_{71}BM$ showed higher J_{sc} while **P2**:$PC_{71}BM$ exhibited higher V_{oc} and demonstrated overall PCE of 4.54% and 4.36%, respectively. The higher value of J_{sc} attributed to the lower band gap and broader absorption profile of **P1** as compared to **P2** and higher V_{oc} for may be attributed the deeper HOMO energy level of **P2** as compared to the **P1**. The PSC processed with DIO/CF showed 5.62% and 5.24%, for **P1**:$PC_{71}BM$ and **P2**:$PC_{71}BM$, respectively, which is attributed the fine morphology adjustment for better exciton dissociation and charge transport in the active layer.

2. Experimental part

2.1. Instruments and characterization methods

^{1}H and ^{13}C NMR spectra of the starting compounds and copolymers were recorded on the spectrometer “Bruker Avance-400” with a working frequency of 400.13 and 100.62 MHz, respectively. IR spectra were recorded by a FT-IR spectrometer “Perkin–Elmer 1720-X”, TGA and DSC analysis was performed on “Per-kin-Elmer TGA-7” and “Perkin–Elmer DSC 7” devices with heating rate of 20 deg/min. The absorption spectra in the range 190–1100 nm were recorded on the spectrophotometer “Varian Cary 50.” The source of the exciting light was a xenon lamp L8253, which is part of the block radiator with optical fiber output radiation “Hamamatsu LC-4.” Cyclic voltammetry measurements were performed on a potentiostat-galvanostat AUTOLAB Type III equipped with standard three-electrode scheme in an acetonitrile solution of 0.1 mol/L tributylammonium perchlorate (n Bu_4NClO_4) at a potential scan rate of 50 mV/s. Films of investigated polymers were deposited on a glass surface coated with ITO and then dried and used as working electrode. Ag/Ag+ and platinum were used as reference and counter electrodes, respectively.

2.2. Synthesis of copolymers P1 and P2

The synthesis and characterization of intermediate monomers used for the synthesis of **P1** and **P2** were described in Supplementary Information.

2.2.1. Synthesis of polymer P1

2,8-Dibromo-4,6-bis(n-octylthiophen-2-yl) benzo[2,1-*b*:3,4-*b*′:5,6-*c*″] trithiophene (10) (0.3964 g, 0.5 mmol) compound 10, 4,7-bis[5-(trimethylstannyl)thiophen-2-yl]-2,1,3-benzothiadiazole ((0.3102 g, 0.5 mmol), $Pd(Ph_3P)_4$ (0.027 g, 0.0234 mmol) and toluene (20 ml) were heated under argon at 110 °C for 48 h. Then 2-bromothiophene (0.02 g) was added and the mixture was stirred at 110 °C for another 5 h. After cooling to r.t. reaction mixture was poured into methanol (200 ml) and filtrated. Polymer was dissolved in $CHCl_3$ and precipitated with methanol. Then it was purified by extraction with methanol, hexane and chloroform in Soxlett apparatus. Yield is 88%. Calc. for $C_{50}H_{46}N_2S_8$,%: C,64.47; H,4.98; N,3.00; S,27.54. Found: C, 64.28; H,4.84; N,3.13; S, 27. 69. ^{1}H NMR (400 MHz, $CDCl_3$, δ, ppm): 8.20–7.40 (6H, Ar), 7.09–6.80 (6H, Ar), 4.25 (4H, alk), 2.30–0.86 (30H, aliph).

2.2.2. Synthesis of polymer P2

P2 was prepared similarly as **P1** using 2,5-dibromo-8-pentadecyl-10*H*-bisthieno[2′,3′:6,7,3″,2″:4,5]indeno[1,2-*d*][1,3] thiazole compound 17 and 4,7-bis[5-(trimethylstannyl)thiophen-2-yl]-2,1,3-benzothiadiazole with 75% yield. Calc. for $C_{29}H_{10}N_4S_5F_8$,%:,C47.93; H,1.39; N, 7.71; S,22.06; F, 20.91 Found:C, 47.98; H,1.27; N, 7.64; S,22.36; F, 20.41. ^{1}H NMR (400 MHz, $CDCl_3$, δ, ppm): 7.74–7.30 (6H, Ar), 7.10–6.89 (29H,alk).

2.3. Device fabrication and characterization

The photovoltaic devices using copolymers as donor and $PC_{71}BM$ as acceptor were fabricated on the indium tin oxide (ITO) coated glass substrate as follow: The ITO coated glass substrates were cleaned continuously in ultrasonic baths containing acetone, detergent, de-ionized water and isopropanol. Then the cleaned ITO glass substrates were dried by high purity nitrogen gas and then treated by UV-ozone for 10 min. The solution of PEDOT:PSS (Clevios PVP Al 4093) was spin coated onto the cleaned ITO glass substrates at 2500 rpm for 30 s and subsequently dried at 100 °C for 20 min in

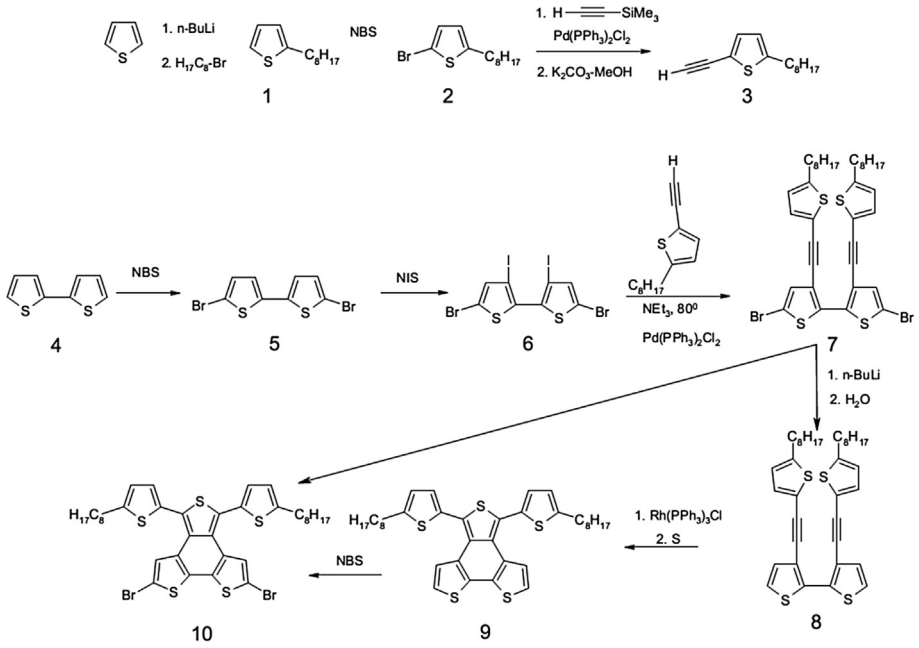

Scheme 1. Synthetic route of monomer **10.**

air. The blends of **P1** or **P2**:$PC_{71}BM$ of different weight ratios were prepared by dissolving the copolymers and fullerene derivatives in chloroform (CF) solution and stirring for about 2 h. For the solvent additive, i.e. DIO/CF, a small amount of DIO (4% by volume) is added to the CF solution. The photoactive layer of **P1** or **P2**:$PC_{71}BM$ (in different ratios with and without solvent additive DIO) was deposited onto the PEDOT:PSS layer by spin coating and then dried in ambient atmosphere. The thickness of the active layer was controlled by the spinning speed and time. The thickness of the active layers was 90–95 nm. The total concentration of mixture of copolymer and $PC_{71}BM$ is 20 mg/ML. Finally, an aluminum (Al) metal top electrode was deposited in vacuum on the active layer at a pressure of less than 10^{-5} torr. The active area of the device was ca. 0.20 mm^2. The current density–voltage (J–V) characteristics were measured on a computer-controlled Keithley 236 source meter unit. A xenon lamp coupled with AM 1.5 optical filter was used as the light source, and the optical power at the sample was 100 mW/cm^2. The incident photon to current conversion efficiency (IPCE) of the devices was measured using a monochromator and xenon lamp as light source and resulting photocurrent was measured with source meter under short circuit condition.

3. Results and discussion

3.1. Synthesis and characterization of P1 and P2

New fused thiophene-containing monomer 2,8-dibromo-4,6-bis(n-octylthiophene-2-yl)benzo[2,1-b:3,4-b′:5,6-c]thrithiophene (**10**) was synthesized by way of consecutive reactions according to Scheme 1.

Including bromination of 2,2′-dithiophene (**4**) with consequent iodization of obtained substance by 5,5′-dibromothiophene (**5**) with the formation of intermediate 3,3′-diiod-5,5′-dibromothiophene (**6**) with the yield of 80%. Bis-ethynyl derivative of 5,5′-dibromo-3,3′-bis(2-(5-n-octylthiophene-2-yl)-2,2′-dithiophene (**7**) was obtained by interaction of the latter with 2 mol of 2-(n-octyl)-

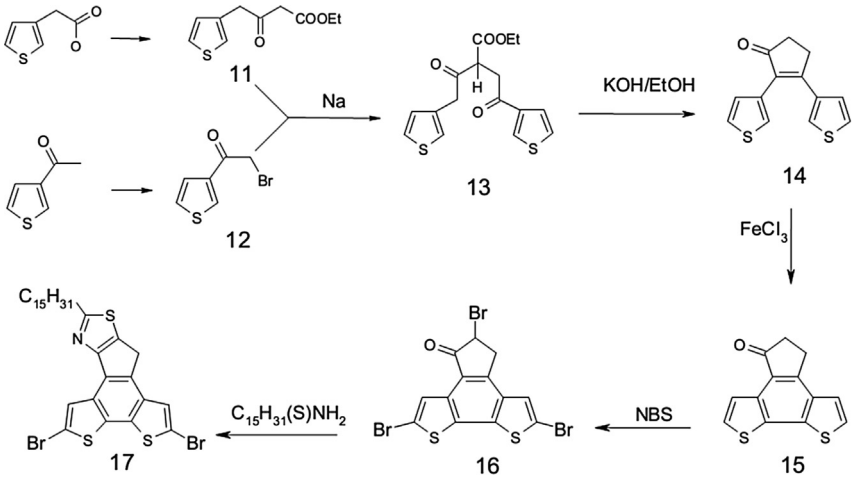

Scheme 2. Synthetic route of monomer **17.**

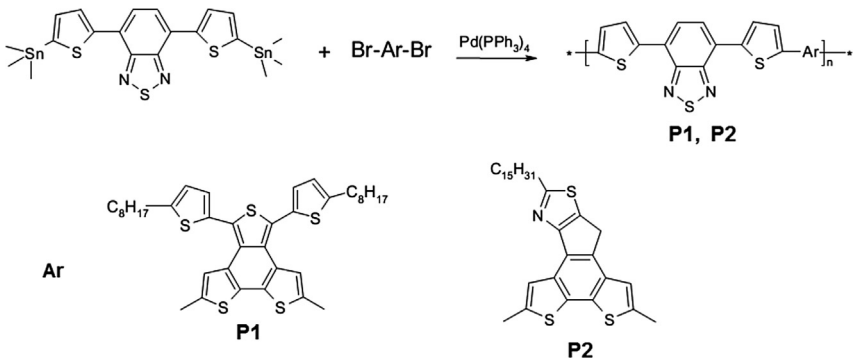

Scheme 3. Synthetic route of copolymers **P1** and **P2.**

5-ethynyl-thiophene in conditions of Suzuki reaction with the yield of 78%. Following cyclization of the product in the presence of Rhodium catalyst and Sulfur in situ lead to the formation of target product – 2,8-dibromo-4,6-bis(5-(2-ethylhexyl) thiophene-2-yl) benzo [2,1-b:3,4-b′:5,6-c″] trithiophene **(10)** with the yield just 10–12%. A yield of 18% was obtained for similar compound in analogous reaction [10]. At the same time compound **8**, without bromine atoms, reacts in similar conditions with the formation of benzotrithiophenes with the yields of 60–70%. In order to increase the yields of final monomers we succeeded to dehalogenate of compound **7** by action of butyllithium with following hydrolysis resulting compound **8** with the yield as high as 91%. Following crystallization of the latter in presence of rhodium catalyst and sulfur in situ leads to formation of 4,6-bisc (5-(2-ethylhexyl)thiophene-2-yl) benzo [2,1-*b*:3,4-*b*′:5,6-*c*″] tritiophene (**9**) with the yield of 73%.

The latter was brominated in the presence of 2 mol excess of bromsuccinimide with the yield of target product 2,8-dibromo-4,6-bis(5-(2-ethylhexyl)-thiophene-2-yl)benzo[2,1-*b*:3,4-*b*′:5,6-*c*″] tritiophene **(10)** 49%). The composition and structure of intermediate compounds 1-9 and target product **10** were confirmed by elemental analysis and NMR ^{1}H ^{13}C. In particular in proton spectra of compound **7** in the range of $\delta = 7.16$, 6.71 and 7.05 ppm two doublets and one singlet were present respectively, corresponding to aromatic protons of thiophene fragments. At $\delta = 2.81–0.87$ ppm appears two triplets typical for CH_2 in direct contact with thiophene ring and terminal CH_3 end alkyl fragment. Ratio of integral intensities of aliphatic and aromatic parts well correspond to the proposed structure. In carbon spectra of aromatic part are present 8 signals, corresponding to 8 non-equivalent aromatic carbon atoms. In the range $\delta = 90 - 87$ ppm 14.3 ppm appear signals, typical for ethynyl and CH_3 groups correspondingly.

In proton spectrum of target product **10** (Fig. S6a) in the range $\delta = 7.22$, 7.09 and 6.89 ppm, resonate one singlet and two doublets relating to aromatic protons of thiophene fragment, in aliphatic range at $\delta = 2.93$ ppm triplet appears, typical for the CH_2 group, directly attached to thiophene ring. In the range $\delta = 1.25–2.00$ ppm signals are present, relating to the rest CH_2 groups of alkyl fragment. At $\delta = 0.91$ ppm triplet resonates, typical for the terminal CH_3 group of alkyl fragment. The ratio of integral intensities of aromatic and aliphatic parts of all intermediate compounds and target

Table 1
Molecular weights and thermal properties of copolymers **P1** and **P2**.

Copolymer	Yield (%)	M_n[a] ($kgmol^{-1}$)	M_w ($kgmol^{-1}$)	PDI	T_g[b] (°C)	T_d[c] (°C)
P1	88	16.4	29.5	1.80	160	393/410[d]
P2	71	11.9	29.8	2.50	205	400/415[d]

[a] Determined by GPC in THF on polystyrene standards.
[b] Determined by DSC at scan rate 20 C/min under nitrogen.
[c] Decomposition temperature, determined by TGA in nitrogen based on 10% weight loss, in numerator – temperature of 10% mass loss in air.
[d] 10% mass loss in Argon atmosphere.

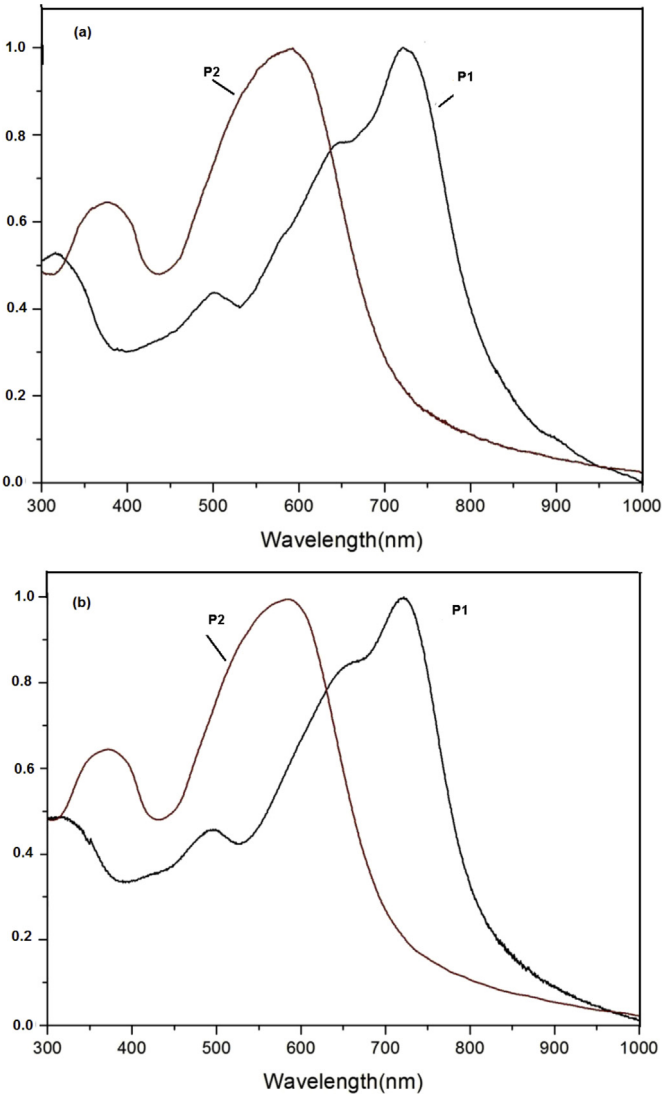

Fig. 1. Normalized UV-vis absorption spectra copolymers **P1** and **P2**, (a) in chloroform solution (1×10^{-5} M) (b) in thin films.

Table 2
Optical and electrochemical properties of copolymers **P1**and **P2**.

Copolymer	λ_{max}^{abs} (nm),solv	λ_{max}^{abs} (nm),film	E_{onset}^{ox} (V)	HOMO (eV)	E_{onset}^{red} (V)	LUMO (eV)	E_g^{ele}(eV)	E_g^{opt} (eV)
P1	499,723	493,734	0.67	−5.15	−0.90	−3.58	1.57	1.51
P2	376,599	370, 610	0.92	−5.40	−0.86	−3.62	1.78	1.73

product well correspond to the proposed structure. In NMR^{13}C **10** (Fig. S6b) in range $\delta = 110–150$ ppm ten signals are present, relating to ten non-equivalent aromatic atoms of carbon in thiophene fragment. Moreover, in aliphatic part, in the range $\delta = 32–14$ ppm resonate 8 signals, relating to eight different aliphatic atoms of carbon.

Synthesis of key monomer 2,5-dibrom-8-heptodecyl-10N-bis-thieno [2′,3′:6,7; 3″,2″:4,5] indeono[1,2-d][1,3] thiazole **(17)** was accomplished according to Scheme 2. Compound 3-oxo-4-thiophene-3-yl-butanoic acid **11** was obtained by acylation of 3-thiopheneacetic acid in the presence of Meldrum acid with the following alcoholysis. Compound 2-brom-1-thiophene-3-yl-ethanone **12** was obtained by bromination of 3-acetylthiophene in the presence of $CuBr_2$. Next stage consisted in equimolar interaction of compound **11** with compound **12** in the presence of Na in absolute benzene with the formation of ethylethere of 3-oxo-2-(2-oxo-2-thiophene-3-yl-ethyl)-4-thiophene-3-yl-butanoic acid **13** with the yield of 87%. Crystallization of compound **13** with formation of 2,3-dithiophene-3-yl-cyclopent-2-enon **14** was carried out in 7% solution of KOH in EtOH:H_2O 1:1 with the yield of 60%. The latter was cyclizated in the presence of $FeCl_3$ with the formation of **15**, following bromination of which lead to compound **16.** Interaction of **16** with aliphatic thioamide leads to the formation of target product **17** with the yield of 71%. The composition and structure of intermediate compounds and target substances were confirmed by elemental analysis data, IR spectroscopy and also NMR ^{1}H and ^{13}C. In particular in IR spectra of compounds **14** and **15** in the range of 1695 cm^{-1} the intensive absorbance line is present, typical for valent vibrations of C]O group, which disappears after conversion into compound **16.** In NMR ^{1}H (Figure S12a) of monomer **17** in weak field range $\delta = 8.16–7.39$ ppm two singlets are present, typical for the protons of thiophene ring in range $\delta = 3.90$ and 3.17 ppm singlet and triplet appear and in range $\delta = 2.01–1.40$ ppm multiplet appears relating to the aliphatic protons of alkyl groups and in range $\delta = 0.90$ the triplet appears, typical for CH_3 groups. The ratio of integral intensities of aromatic part to aliphatic of all intermediates and target compounds well correspond to the proposed. In NMR^{13}C **17** (Fig. S12b) in range $\delta = 110–180$ ppm thirteen signals are present, relating to thirteen non-equivalent aromatic atoms of carbon in thiophene fragment and in aliphatic part in the range $\delta = 38–14$ ppm resonate signals, relating to different aliphatic atoms of carbon.

The new low band gap donor −acceptor (D–A) copolymers **P1** and **P2** with quinoid character of π-conjugation and strong alternation of donor-acceptor fragments, obtained under conditions of cross coupling Stille reaction according to Scheme 3. Polycondensation was carried out in Argon atmosphere in toluene at 110° C during 48 h, using tetrakis (triphenylphosphine) palladium as a catalyst. As the electron-donor fragment in The copolymers **P1** and **P2** consist same 4,7-[bis-trimethylstannyl-(thiophen-2-yl)-2,1,3-benzthiadiazole acceptor unit and different donor moiety i.e. 2,8-dibromo-4,6-bis(n-octylthiophene-2-yl) benzo[2,1-*b*:3,4-*b*′:5,6-*c*″] trithiophene (monomer **10**) and 2,5-dibromo-8-pentadecyl-10*H*-bis-thieno [2′,3′: 6,7, 3″, 2″:4,5] indeno [1,2-*d*][1, 3] thiazole (monomer **17**), respectively.

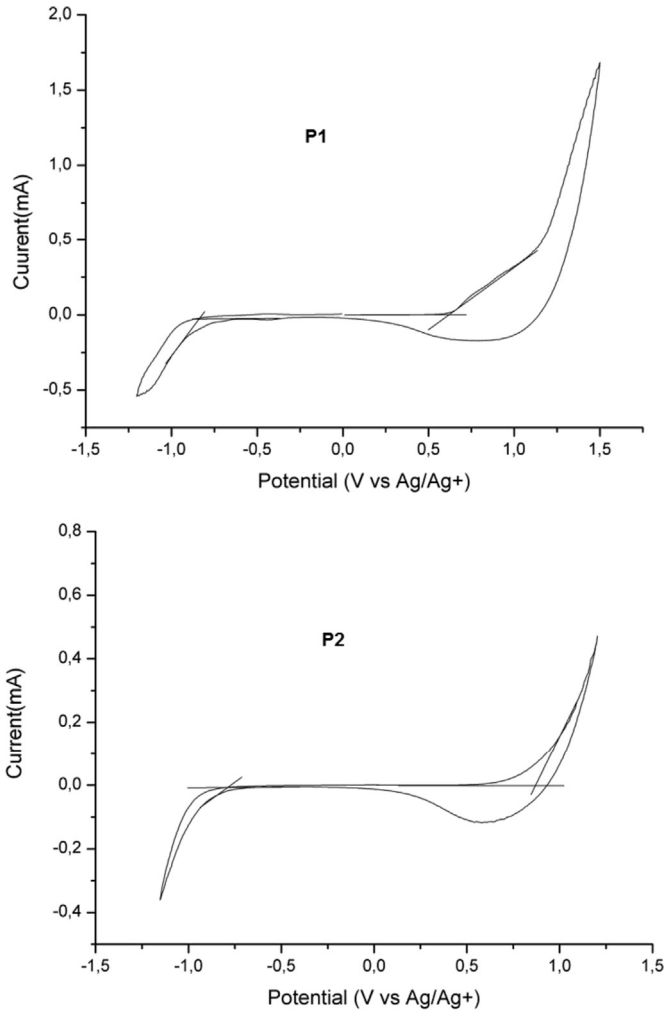

Fig. 2. Cyclic voltammetry curves of polymers **P1 and P2** films on platinum electrode in 0.1 mol/L Bu_4NClO_4 in CH_3CN solution at scan rate 50 mVS^{-1}.

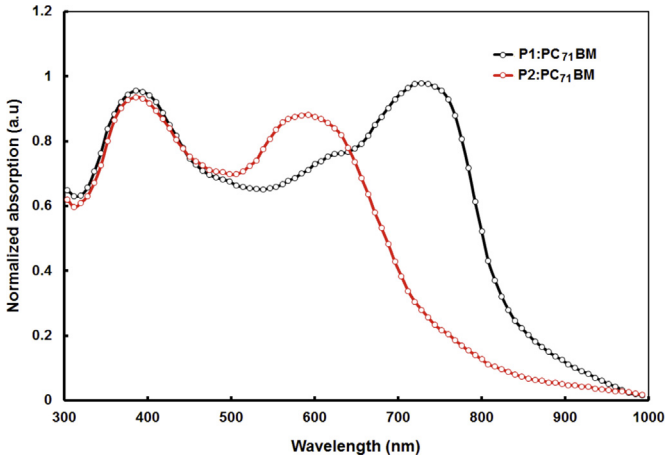

Fig. 3. Normalized absorption spectra of **P1**:$PC_{71}BM$ and **P2**:$PC_{71}BM$ thin films.

Table 3
Photovoltaic parameters of organic polymer photovoltaic devices based on **P1**:$PC_{71}BM$ and **P2**:$PC_{71}BM$ active layer.

Active layer	J_{sc} (mA/cm^2)	V_{oc} (V)	FF	PCE (%)	μ_h (cm^2/Vs)	μ_e (cm^2/Vs)	μ_e/μ_h
P1:$PC_{71}BM$[a]	10.96	0.74	0.56	4.54	9.56×10^{-6}	2.46×10^{-4}	23.51
P2:$PC_{71}BM$[a]	9.12	0.92	0.52	4.36	7.54×10^{-6}	2.40×10^{-4}	31.83
P1:$PC_{71}BM$[b]	12.95	0.70	0.62	5.62	9.64×10^{-5}	2.52×10^{-4}	2.61
P2:$PC_{71}BM$[b]	10.88	0.86	0.56	5.24	7.42×10^{-5}	2.56×10^{-4}	3.45

[a] CF cast.
[b] DIO/CF cast.

Obtained polymers **P1** and **P2** were purified from the residues of catalysts, tin-organic and low molecular impurities by two-fold re-sedimentation from solution in methanol and following extraction with methanol, hexane and chloroform. Yield of polymer **P1** and **P2** was 88% and 71%, respectively. The composition and structure of polymers **P1** and **P2** were confirmed by elemental analysis data and NMR ^{1}H and NMR^{13}C spectroscopy.

The thermal properties of the **P1** and **P2** were investigated via DSC and TGA methods and the data were summarized in Table 1. The glass transition temperature of P1 and P2 estimated from DSC measurement are 160° and 205°°C, respectively. Both the co-polymers have the sufficient high thermal stabilities. The temperature of 5% wt loss of the copolymer in nitrogen i.e. $T_{5\%}$ are 410° and 415 °C for **P1** and **P2**, respectively. These results show that the copolymers show thermal stabilities sufficiently high for the use in polymer solar cells.

3.2. Optical and electrochemical properties

The UV-visible absorption spectra of **P1** and **P2** were investigated in dilute chloroform solution and in thin films and shown in Fig. 1a and b, respectively and detail data were summarized in Table 2. As shown in Fig. 1a and b both the polymers showed two absorption peaks, which is a typical feature of D–A polymers. The absorption peak in shorter wavelength region originated from the π–π^* transition of the polymer main chain, and the absorption in the longer wavelength region, mainly due to the charge transfer between the donor and acceptor units present in the D–A polymer [11]. The absorption spectra of both co-polymers in thin film were similar to their corresponding solution spectra, with slight red shifts of their absorption maximum, due to the enhanced intermolecular electronic interactions in the solid state. The optical bandgap of these polymers was estimated from the onset absorption edge of absorption spectra

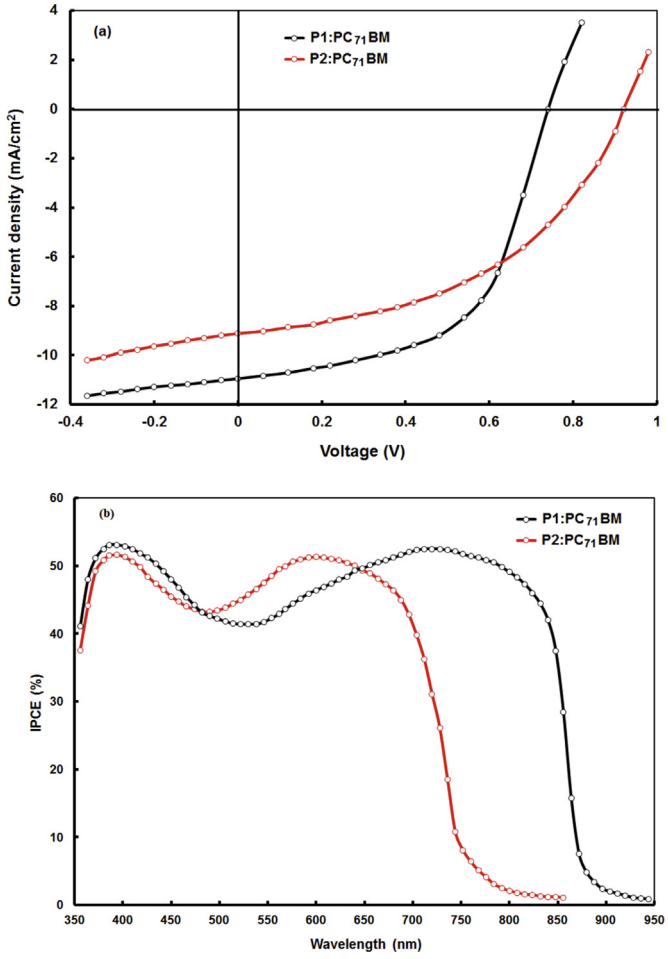

Fig. 4. (a) Current-voltage (J–V) characteristics under illumination and (b) IPCE spectra of devices based on **P1**:$PC_{71}BM$ and **P2**:$PC_{71}BM$ active layer processed with CF solvent.

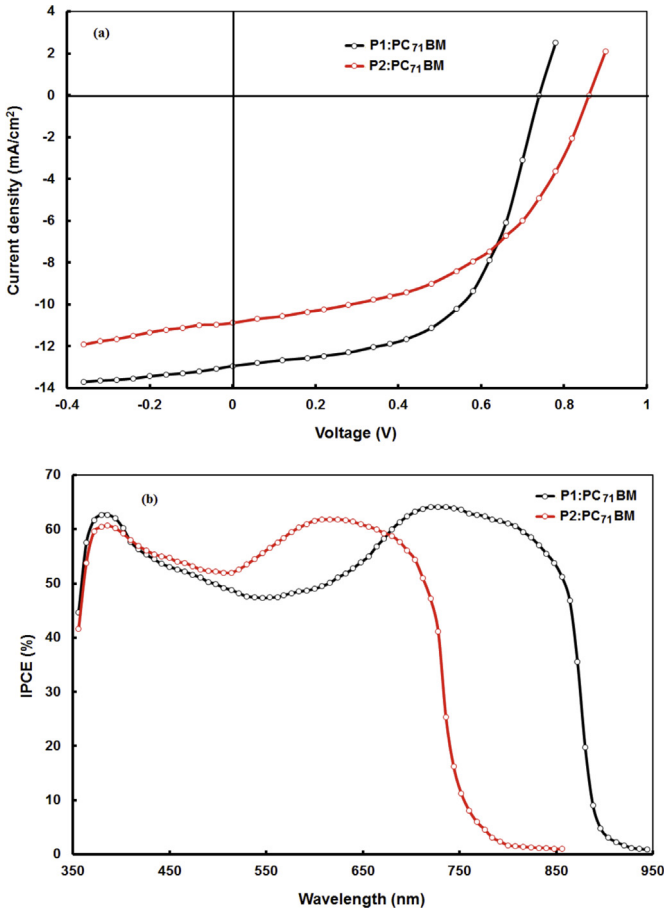

Fig. 5. (a) Current-voltage (J–V) characteristics under illumination and (b) IPCE spectra of devices based on **P1**:$PC_{71}BM$ and **P2**:$PC_{71}BM$ active layer processed with DIO (4 v %)/CF solvent.

of their in film and is about 1.51 eV and 1.73 eV for **P1** and **P2**, respectively.

The energy levels of the copolymers were examined by cyclic voltammetry in acetonitrile with 0.1 M tetrabutylammonim perchlorate (Bu_4NClO_4) at scan speed of 50 mV/s. Platinum electrode was used as the counter-electrode, Ag/Ag^+ in 0.1M solution of $AgNO_3$ as reference electrode, and Fc/Fc^+ as an external standard. The results of cyclic voltammograms are presented in Fig. 2a and b in data were summarized in Table 2. Both the copolymers exhibit reversible or partly reversible redox properties.

The electrochemical properties of polymers were investigated by cyclic voltammetry measurements and shown in Fig. 2. The HOMO and LUMO energy levels were calculated from their onset oxidation potential and onset reduction potentials according to the following expressions:

$$E_{HOMO} = -q(E^{ox}_{onset} + 4.48)eV$$
$$E_{LUMO} = -q\left(E^{red}_{onset} + 4.48\right)eV$$

The HOMO energy level of **P1** (−5.15 eV) is higher than that of **P2** (−5.40 eV). This can be easily understood because donating ability of 2,8-dibromo-4,6-bis(n-octylthiophene-2-yl)benzo[2,1-b:3,4-b′:5,6-c] thrithiophene in **P1** is stronger than that 2,5-dibromo-8-pentadecyl-10*H*-bis-thieno [2′,3′: 6,7, 3″, 2″:4,5] indeno [1,2-*d*][1, 3] thiazol in **P2**, since the strong donating unit in the donor polymer raises the HOMO energy level. The LUMO levels of **P1** and **P2** are −3.58 eV and −3.62 eV, respectively, the LUMO offsets between the donor polymers and $PC_{71}BM$ (−4.1 eV) are larger than 0.3 eV, which is sufficient for effective exciton dissociation [4a]. The electrochemical bandgap of **P1** and **P2** are 1.57 eV and 1.76 eV and the trend is consistent with the optical bandgap within the experimental error. The deeper HOMO energy level of both copolymers than that of P3HT favors the high value of V_{oc} when used as donor for the fabrication of BHJ polymer solar cells.

3.3. Photovoltaic properties

We have investigated the photovoltaic properties of the copolymers in BHJ solar cells having the sandwich structure ITO/PEDOT:PSS/copolymer:$PC_{71}BM$ (1:2)/Al with the photoactive layers having been spin coated from chloroform solutions of copolymer and $PC_{71}BM$. After testing several compositions, we found that the optimized weight ratio of the copolymer and $PC_{71}BM$ was 1:2. The normalized absorption spectra of **P1**:$PC_{71}BM$ and **P2**:$PC_{71}BM$ thin films were shown in Fig. 3. It can be seen from these spectra that the blend films exhibited the absorption spectra of both copolymer and $PC_{71}BM$.

The J–V curves under illumination (AG1.5100 mW/cm^2) of these PSCs based with **P1** or **P2**:$PC_{71}BM$ (1:2) blend are shown in Fig. 4 and corresponding photovoltaic parameters are summarized in Table 3. The maximal PCE of 4.54% with V_{oc} of 0.74 V, J_{sc} of 10.96 mA/cm^2 and FF of 0.56 was obtained for **P1**:$PC_{71}BM$ device, while **P2**:$PC_{71}BM$ based device showed a PCE of 4.36% with J_{sc} of 9.12 mA/cm^2, V_{oc} of 0.92 V and FF of 0.52. The higher value of V_{oc} of for the device with **P2** may be due to deeper HOMO energy level of **P2** as compared to **P1** [12]. The J_{sc} of the devices incorporating the blend of **P1** and **P2** with $PC_{71}BM$ were 10.96 and 9.12 mA/cm^2, respectively. The higher value of J_{sc} with **P1** may be its broader absorption profile and high hole mobility as compared to that for **P2** [13].

The incident photon to current conversion efficiency (IPCE) spectrum of the optimized device were investigated and shown in Figure. The IPCE spectra of devices closely resembles to the absorption spectra of respective blended active layers, indicating both copolymers and $PC_{71}BM$ contributed to the exciton generation and thereby in photocurrent generation. High IPCE value over 40% in a broad range from 350 to 680 nm and 350–840 nm for **P2**:$PC_{71}BM$ and **P1**:$PC_{71}BM$, respectively, was observed. The maximum IPCE of 53% at 384 nm and 725 nm for **P1**:$PC_{71}BM$ and 51% at 386 nm and 608 nm for **P2**:$PC_{71}BM$. Obviously, the **P1**:$PC_{71}BM$ active layer

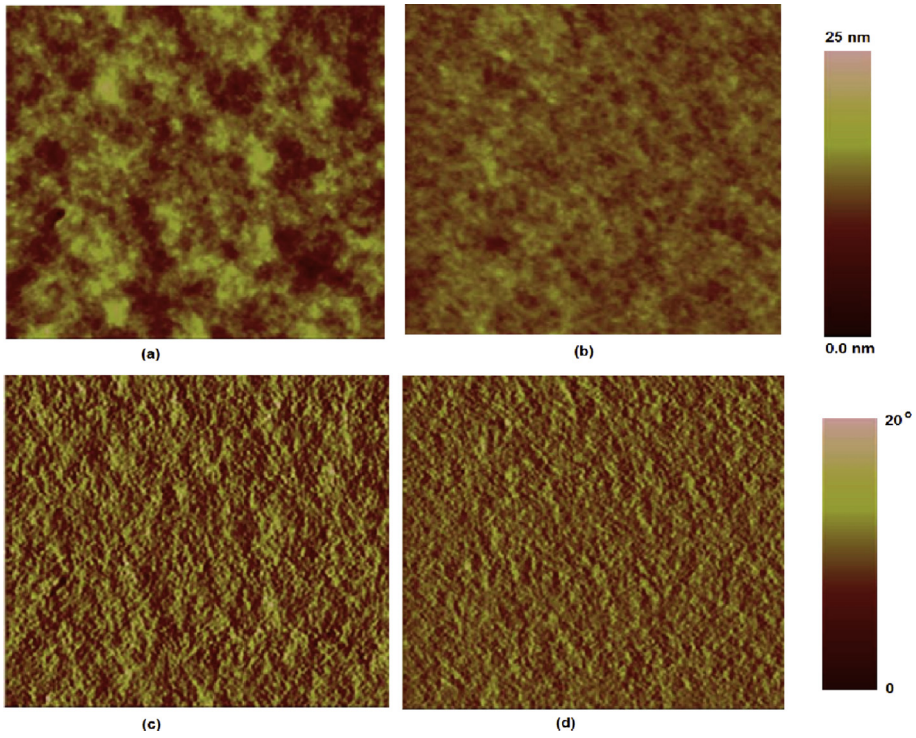

Fig. 6. AFM morphology images (a, b) and phase images (c, d) of **P1**:$PC_{71}BM$ blend films processed with CF and DIO/CF as solvents, image size 5 μm × μm.

based device shows higher values of IPCE as well as broader IPCE spectra compared to **P2**:$PC_{71}BM$ based device, leading to higher value of J_{sc} for former device. The J_{sc} value estimated from integration of IPCE spectra for **P1**:$PC_{71}BM$ and **P2**:$PC_{71}BM$ based device was about 10.75 mA/cm^2 and 9.04 mA/cm^2, respectively. These values are closely resembled with the measured values from J–V characteristics under illumination.

The over all PCE of the BHJ polymer solar cells based on above copolymers is still low and may be due to the low fill factor and J_{sc}. The performance of the polymer solar cells based on BHJ active layer requires the optimization of molecular scale order and its nanoscale domain structure [14]. Many techniques have been employed for the optimization of BHJ film active layer [15], including solvent choice and thermal annealing [16] or vapor annealing [17]. Recently use of high boiling point solvent additive in the host solvent has have employed to achieve the high PCE without thermal annealing and have become popular [18]. To further improve the PCE of the polymer solar cells using **P1** and **P2** as donor and PCBM as acceptor, we have used DIO (4% v) as solvent additive i.e. DIO (4 %v)/CF. The J–V characteristics under illumination and IPCE spectra of these device were shown in Fig. 5 and the photovoltaic data were complied in Table 3. The PCE have been enhanced up to 5.62% and 5.24% for **P1**:$PC_{71}BM$ and **P2**:$PC_{71}BM$, respectively. The increase in PCE is due to the higher values of both J_{sc} and FF.

The J_{sc} of the polymer solar cells processed on the solvent additive has been improved which is in agreement with the increase in the IPCE values (Fig. 5a). Since the J_{sc} of a polymer solar cells depends upon the exciton dissociation into electrons and holes in the active layer and their charge transport towards the respective electrodes. We have investigated the surface morphology of the BHJ active layer films processed with and without DIO additives using atomic force microscopy (AFM) for blends. AFM height and phase images of **P1**:$PC_{71}BM$ are shown in Fig. 6. Similar image were also observed for **P2**:$PC_{71}BM$ blends. The average surface roughness measured from the topographic images were 3.44 nm, 2.14 nm, 2.76 nm and 1.45 nm for **P2**:$PC_{71}BM$ (CF cast), **P2**:$PC_{71}BM$ (DIO/CF cast), **P1**:$PC_{71}BM$ (CF cast) and P1$PC_{71}BM$ (DIO/CF cast), respectively. The phase images of the active layer films show uniform D–A interpenetrating networks with appropriate domain sizes (30–35 nm for CF cast and 20–25 nm for DIO/CF cast respectively). The increased value of J_{sc} for the devices processed with solvent additives as compared CF cast, may be due the reduced domain size and improved phase separation, enhancing the exciton dissociation and charge transport.

We further investigated the effect of solvent additives on the charge transport properties of active layers using space charge limited current (SCLC) method. The hole only ITO/PEDOT:PSS/blend/Au and electron devices ITO/Al/blend/Al were fabricated to estimate the hole and electron mobilities in active layers, using the dark J-V characteristics in forward bias (Fig. 7). The mobilities were extracted by fitting the J-V curves using Mott-Gurney relationship [18]:

$$J = \frac{9}{8}\varepsilon_o \varepsilon_r \mu \frac{V^2}{d^3}$$

where J is the current density, d is the film thickness of the active layer, μ is the charge carrier mobility, ε_r is the relative dielectric constant of the transport medium, εo is the permittivity of free space (8.55×10^{-12} F/m), V is the internal voltage in the device, i.e. $V = V_{appl} - V_{bi}$, V_{appl} is the applied voltage to the device and V_{bi} is the built in voltage due to the relative work function difference of the two electrodes. The values of hole and electron mobilities were also complied in Table 3. As shown in Table 3, the hole mobilities for

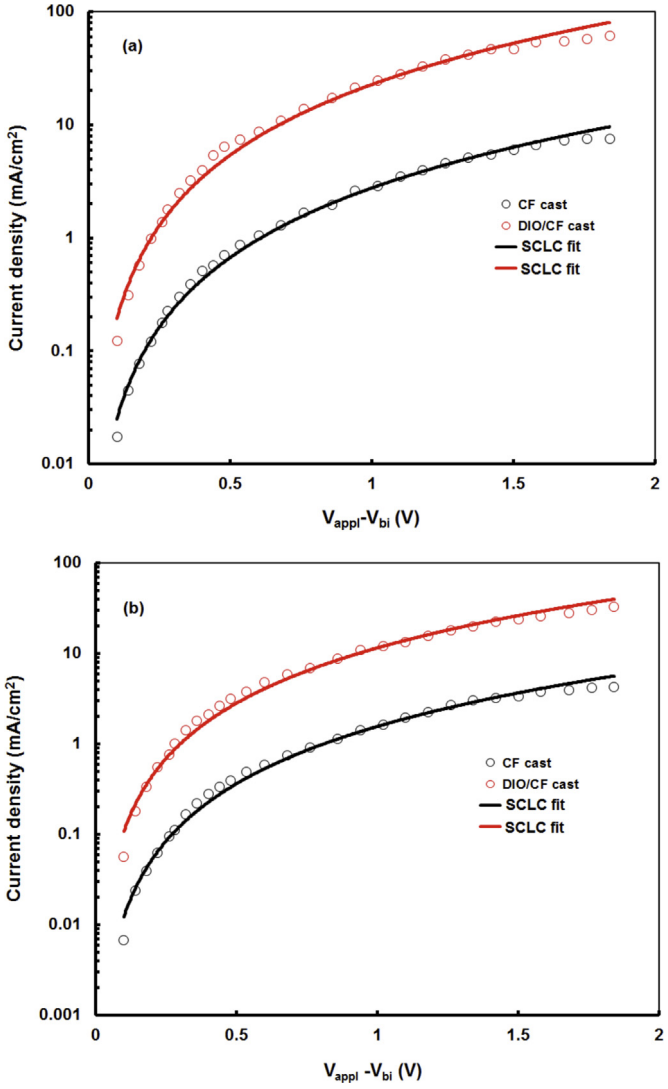

Fig. 7. Current –voltage (J–V) characteristics of the hole only devices based on (a) **P1**:$PC_{71}BM$ and (b) **P2**:$PC_{71}BM$ blend active layers processed from CF and DIO/CF solvents. Solid lines are SCLC fit.

CF cast **P1**:$PC_{71}BM$ and **P2**:$PC_{71}BM$ are about 9.56×10^{-6} cm^2/V and 7.54×10^{-6} cm^2/V, respectively. However, using the solvent additives, the hole mobilities has been increased significantly up to 8.64×10^{-5} and 7.42×10^{-5} cm^2/V, for **P1**:$PC_{71}BM$ and **P2**:$PC_{71}BM$ blend, respectively. The solvent additive only slightly affects the electron mobility in the active layers, since the solvent additive does not effect the crystallinity of the $PC_{71}BM$ phase. The higher hole mobility that resulted from the solvent additives permitted the holes to travel faster during the charge transport processes, resulting higher J_{sc} [18,19]. Moreover, the devices processed with the solvent additives show relatively well balanced mobility compared to those without solvent cast devices. The more balanced mobility contributes to higher J_{sc} and FF because of accumulated SCLC charges and hence recombination processes are reduced by the increase in hole mobility and enhance charge collection efficiency [20].

4. Conclusions

We designed and synthesized two low band gap D–A copolymers **P1** and **P2** with same benzothiadiazole acceptor unit and

different fused thiophene donor units. The optical absorption range and energy levels of the copolymers were easily tuned thought the introduction of different donor units. These copolymers showed favorable electrochemical energy levels and are compatible with the $PC_{71B}M$ for efficient exciton dissociation and charge transfer. The device based on **P1**:$PC_{71}BM$ showed higher J_{sc} while **P2**:$PC_{71}BM$ exhibited higher V_{oc} and demonstrated overall PCE of 4.54% and 4.36%, respectively. The higher value of J_{sc} attributed to the lower band gap and broader absorption profile of SB20 as compared to **P2** and higher Voc for may be attributed the deeper HOMO energy level of **P2** as compared to the **P1**. The PSC processed with DIO/CF showed 5.62% and 5.24%, for **P1**: $PC_{71}BM$ and **P2**:$PC_{71}BM$, respectively, which is attributed the fine morphology adjustment for better exciton dissociation and charge transport in the active layer.

Acknowledgments

This work is supported by the Russian foundation for basic research (grant number 13-03-92709-IND_a, grant number 14-03-92003, grant number 13-03-91166) and DST, Government of India (DST-RFBR joint research project) grant number INT/RUS/RFBR/P-151. We are thankful to Department of Physics, LNMIT, Jaipur and Material Research Laboratory, MNIT, Jaipur for providing the facilities of device fabrication and characterization. FCC thanks the support from Ministry of Science and Technology of Taiwan.

Appendix A. Supplementary data

Supplementary data related to this article can be found at http://dx.doi.org/10.1016/j.polymer.2015.03.058.

References

[1] (a) Yu G, Gao J, Hummelen JC, Wudl F, Heeger AJ. Science 1995;270:1789–91;
(b) Arias AC, MacKenzie J, McCulloch I, Rivnay J, Salleo A. Chem Rev 2010;110:3–24;
(c) Li G, Zhu R, Yang Y. Nat Photonics 2012;6:153–61;
(d) Krebs FC, Espinosa N, Hosel M, Søndergaard RR, Jørgensen M. Adv Mater 2014;26:29–39;
(e) Espinosa N, Hosel M, Jørgensen M, Krebs FC. Energy Environ Sci 2014;7:855–66;
(f) Søndergaard RR, Hosel M, Krebs FC. J Polym Sci Part B, Polym Phys 2013;51:16–34.
[2] (a) Small CE, Chen S, Subbiah SJ, Amb CM, Tsang SW, Lai TH, et al. Nat Photonics 2011;6:115–20;
(b) Lu L, Luo Z, Xu T, Yu L. Nano Lett 2013;13:59;
(c) He Z, Zhong C, Huang X, Wong WY, Wu H, Chen L, et al. Adv Mater 2011;23:4636–43;
(d) Cabanetos C, El Labban A, Bartelt JA, Douglas JD, Mateker WR, Frechet JM, et al. J Am Chem Soc 2013;135:4656–9;
(e) Dou L, Chen CC, Yoshimura K, Ohya K, Chang WH, Gao J, et al. Macromolecules 2013;46:3384–90;
(f) Li X, Choy WC, Huo L, Xie F, Sha WE, Ding B, et al. Adv Mater 2012;24:3046–952;
(g) He Z, Zhong C, Su S, Xu M, Wu H, Cao Y. Nat Photonics 2012;6:593–7;
(h) Yang T, Wang M, Duan C, Hu X, Huang L, Peng J, et al. Energy Environ Sci 2012;5:8208–14;
(i) Chen HC, Chen YH, Liu CC, Chien YC, Chou SW, Chou PT. Chem Mater 2012;24:4766–72.
[3] You J, Dou L, Yoshimura LK, Kato T, Ohya K, Moriarty T, et al. Nat Commun 2013;4:1446.
[4] (a) Brabec CJ, Cravino A, Meissner D, Sariciftci NS, Fromherz T, Rispens MT, et al. Adv Funct Mater 2001;11:374–80;
(b) Yang B, Guo FW, Yuan YB, Xiao ZG, Lu YZ, Dong QF, et al. Adv Mater 2013;(25):572–7;
(c) Yuan JY, Zhai ZC, Dong HL, Li J, Jiang ZQ, Li YY, et al. Adv Funct Mater 2013;23:885–92.
[5] (a) Seo JH, Kim D, Kwon S, Song M, Choi M, Ryu SY, et al. Adv Mater 2012;24:4523;
(b) Gao C, Wang L, Li X, Wang H. Polym Chem 2014;5:5200–10.
[6] Cheng YJ, Yang SH, Hsu CS. Chem Rev 2009;109:5868;
(b) Gao F, Inganäs O. Phys Chem Chem Phys 2014;16:20291–304.
[7] (a) Guo X, Punired SR, Baumgarten M, Pisula W, Müllen K. J Am Chem Soc 2012;134:8404–7;
(b) Guo X, Puniredd SR, Baumgarten M, Pisula W, Müllen K. Adv Mater 2013;25:5467–72.
[8] (a) Szarko JM, Guo J, Liang Y, Lee B, Rolczynski BS, Strzalka J, et al. Adv Mater 2010;22:5468–72;
(b) Wang E, Hou L, Wang Z, Ma Z, Hellström S, Zhuang W, et al. Macromolecules 2011;44:2067–73;
(c) Yiu AT, Beaujuge PM, Lee OP, Woo CH, Toney MF, Frechet JM. J Am Chem Soc 2012;134:2180–5;
(d) Lei T, Dou JH, Pei J. Adv Mater 2012;24:6457–61.
[9] (a) Zhou H, Yang L, You W. Macromolecules 2012;45:607–32;
(b) Zhao X, Yang D, Lv H, Yin L, Yang X. Polym Chem 2013;4:57–60;
(c) Lan SC, Yang PA, Zhu MJ, Yu CM, Jiang JM, Wei KH. Polym Chem 2013;4:1132–40;
(d) Kashiki T, Kohara M, Osaka I, Miyazaki E, Takimiya K. J Org Chem 2011;76:4061–70;
(e) Nielsen CB, Ashraf RS, Schroeder BC, D'Angelo P, Watkins SE, Song K, et al. Chem Commun 2012;48:5832–4.
[10] Zhang Y, Zou J, Cheuh CC, Yip HL, Jen AKY. Macromolecules 2012;45:5427–35.
[11] (a) Mühlbacher D, Scharber M, Morana M, Zhu Z, Waller D, Gaudiana R, et al. Adv Mater 2006;18:2884–9;
(b) Zoombelt AP, Fonrodona M, Turbiez MGR, Wienk MM, Janssen RAJ. J Mater Chem 2009;19:5336–42.
[12] DeLongchamp DM, Kline RJ, Herzing A. Energy Environ Sci 2012;5:5980–93.
[13] Li G, Shrotriya V, Yao Y, Huang J, Yang Y. J Mater Chem 2007;17:3126–40.
[14] Berson S, De Bettignies R, Bailly S, Guillerez S. Adv Funct Mater 2007;17:1377–84.
[15] Li G, Shrotriya V, Huang J, Yao Y, Moriarty T, Emery K, et al. Nat Mater 2005;4:864–8.
[16] (a) Peet J, Kim JY, Coates NE, Ma WL, Moses D, Heeger AJ, et al. Nat Mater 2007;6:497–500;
(b) Moulé AJ, Meerholz K. Adv Funct Mater 2009;19:3028–36;
(c) Liao HC, Ho CC, Chang CY, Jao MH, Darling SB, Su WF. Mater Today 2013;16:326–36.
[17] Gao J, Dou L, Chen W, Chen CC, Guo X, You J, et al. Adv Energy. Mater 2014;4:1300739.
[18] Mihailetchi VD, Koster LJA, Blom PWM, Melzer C, de Boer B, van Duren JKJ, et al. Adv Funct Mater 2005;15:795–801.
[19] Lin Y, Li Y, Zhan X. Adv Energy. Mater 2013;3:724–8.
[20] (a) Hai J, Yu W, Zhao B, Li Y, Yin L, Zhu E, et al. Polym Chem 2014;5:1163;
(b) Ge L, Gu J, Yu j, Zhu E, Hai J, Bian, L, et al, Phys Chem Chem Phys. http://dx.doi.org/10.1039/c5cp00349k.